Manufacture and characterization of carbonated lightweight aggregates from waste paper fly ash

Bader Bouzar, Yannick Mamindy-Pajany

Manufacture and characterization of carbonated lightweight aggregates from waste paper fly ash

Bader Bouzar [a, b, *], Yannick Mamindy-Pajany [a, b]

[a] IMT Nord Europe, Institut Mines-Télécom, Centre for Materials and Processes, Environnement, F-59000 Lille, France.

[b] Univ. Lille, Univ., ULR 4515 – LGCgE, Laboratoire de Génie Civil et géo-Environnement, F-59000 Lille, France.

*Corresponding author (Bader Bouzar): bader.bouzar@imt-nord-europe.fr (ORCID: 0000-0002-1181-0258)

Author: Yannick Mamindy-Pajany: yannick.mamindy@imt-nord-europe.fr

ABSTRACT

The combustion of biomass and waste paper sludge in a fluidized bed is ecologically profitable. However, a large amount of by-product with high hydraulic reactivity is produced and is considered as wastes. Most of the time the waste paper fly ash (WPFA) goes to landfills, therefore new utilization methods are necessary. In some countries, the high content of metallic and metalloids trace elements (MMTE) in WPFA, more specifically Barium (Ba) and Lead (Pb) makes its valorization difficult. In this paper, the Lightweight Aggregates (LWA) was produced from WPFA by granulating with water in high-intensity granulator. Since WPFA is rich in CaO, the addition of water promotes rapid setting and hydration compared to other types of ash. In this study, different granulation parameters were investigated, such as the rotation modes between the steel pan and the impeller, the rotation speed of the steel pan, the granulation time, in order to improve the mass percentage of the targeted LWA (2-16 mm). In order to evolve the immobilization potential of Ba and Pb, a carbonation process was performed, exposing the manufactured LWA to pure carbon dioxide (CO_2) gas at laboratory scale. The physical, morphological, thermal and mechanical characterizations were performed on LWA for use in mortars, concretes or civil engineering constructions.

Results have demonstrated the influence of the rotation mode between the steel pan and the on the distribution of WPFA inside the steel pan and the change in the growth rate of the granules can be observed. Increased density and improved compressive strength with low porosity and water absorption were also found in LWA after carbonation. This was due to the occurrence of both a carbonation reaction and a hydration reaction. Furthermore, the results of thermogravimetry and SEM-EDS confirmed the formation of hydrated phases (ettringite, carboaluminates), also the formation of calcite in the pores and the external surface of the LWA. Regarding environmental aspects, the results have revealed that Ba and Pb were well immobilized in the solid matrix after carbonation.

Keywords: *Waste paper fly ash, accelerated carbonation, lightweight aggregates, Stabilization, Metallic and metalloids trace elements.*

Abbreviations

Waste paper fly ash (WPFA)

Lightweight aggregates (LWA)

Metallic and metalloids trace elements (MMTE)

Biomass fly ash (BFA)

Loss on Ignition (LOI)

Scanning Electron Microscopy with Energy Dispersive Spectroscopy (SEM-EDS)

1.Introduction

In France, the annual production of fly ash (FA) from paper sludge and waste biomass combustion has been estimated to be about 120 000 tons**.** Two of the twelve paper mills equipped with biomass boilers use paper mill sludge as a substitute for biomass up to 60% [1]. The physical-chemical properties of this ash depend mainly on the combustibles used by the boilers of the paper production and/or recycling plants. However, new wastes (pulp processing sludge and de-inking sludge) are produced during recycling operations, creating new challenges. For example, paper manufacturers have found combustible material for their boilers in these sludges (with high calorific value), which constitutes an

important recovery channel limiting the need for disposal [1]. When these residues are co-incinerated with biomass, new waste is generated: Waste Paper Fly Ash (WPFA).

The amount of WPFA generated worldwide will likely continue to increase in the near future. The increasing demand for energy and the polluting nature of current fossil fuel sources demonstrate the need for new energy technologies, which offer greater efficiency with minimal environmental damages [2]. The process of energy production from biomass, which is already widely available, is considered to have a near-zero carbon dioxide (CO_2) impact [3], because the emissions produced during its use neutralize the CO_2 fixed in the biomass during its growth. The use of biomass for energy is based on the idea that it is a carbon-neutral fuel and will help reduce greenhouse gas emissions. The combustion of biomass for heat and power produces ash composed mainly of inorganic elements naturally present in the biomass. This FA is often disposed of in landfills, which is currently becoming unattractive due to costs and may not be possible in the future due to EU (European Union) policy instruments for a circular economy [4].

WPFA is different from coal FA because it is derived from different fuels [5]. WPFA is an industrial by-product of the energy industries and has significant potential for use as a pozzolanic mineral admixture and as an activator or binder for cement composite materials. Currently, WPFA is not yet widely used commercially, unlike coal FA. Most WPFA produced by power plants is either landfilled or recycled on fields or forests, and often this happens without any form of control [6]. The WPFA differs from coal FA primarily in its chemistry and mineralogy [7]. Compared to coal, WPFA contains a high content of calcium oxide (CaO), silica (SiO_2) and alumina (Al_2O_3) and low content of iron oxide (Fe_2O_3) [8]. The presence of unreacted lime gives the WPFA a high alkalinity, and the WPFA has a high chloride (Cl) content (typically 10-20%) which has a high complexing capacity for several metallic and metalloids trace elements (MMTE). Both of these factors have resulted in an increased potential for leaching of amphoteric trace elements, which is important when it comes to landfills. The WPFA are produced from wastes paper sludge and waste biomass, it contains high levels of hazardous elements such as Barium (Ba), Plomb (Pb) and Chlorides. The high levels of trace elements in the WPFA limit its reuse. This forces energy producers to transport the WPFA to landfills, leading to

greater costs and environmental risks. A workaround would be recovering of MMTE from WPFA [9]–[12]. However, this is not economically or technologically feasible. For all these reasons, sustainable management must be established. The amount of FA is increasing and so is the cost of disposal. The development of innovative methodologies to convert WPFA into useful materials is essential to support the increasing use of biomass for energy production [7]. Therefore, granulation/carbonation is the next better option.

Raw materials used to produce artificial aggregates are becoming depleted and society is increasingly concerned about preserving natural resources by producing alternative materials. Therefore, there is a growing interest in using other natural sources such as sediments and FA for the production of artificial aggregates. Several studies have shown that in the field of civil engineering, FA can be used as a substitute for traditional aggregates, such as the use of coal FA or biomass in the manufacture of lightweight aggregates (LWA). Chen et al [13], developed new aggregates based on FA and showed that they can replace 15% natural aggregates in concrete. In another study, Andrade et al [14], produce aggregates by heat treatment of bottom ash, the results show that the higher the percentage of bottom ash aggregate in concrete, the worse the performance regarding moisture transport, However, the mechanical properties remain similar. However, the results of Liu et al [15], showed that natural sand aggregates can be replaced by plastic granules. The increase in the percentage of plastic granules in concrete results in a higher energy absorption capacity compared to ordinary concrete. Thus, the impact resistance of recycled plastic concrete materials was higher than that of ordinary concrete. Some studies [16], [17] use thermally modified FA as aggregates in particulate form, the result show that the strength and specific gravity of all aggregates decreased with increasing the FA content at the highest temperature. The dense structure of the aggregates can be the factor responsible for increasing the mechanical strength and specific gravity as well as decreasing the water absorption. Alqahtani et al [18], use a thermoplastic matrix (linear low-density polyethylene) containing fillers: sand, quarry, red sand/dunes, FA to produce LWA. The aggregate produced was lightweight, with a density ranging from 510 to 750 kg/m^3 and absorption of from 2.7 to 9.81%. Other properties such as strength and thermal conductivity were comparable to aggregates of similar density. Finally, Franus et al [19], have

manufactured lightweight aggregates from fly ash, using a new method that replaces burner furnaces with microwave furnaces, The results concluded that compressive strength of lightweight aggregates increases with longer microwave heating time.

Agglomeration, or granulation, is defined as a process of increasing the average size of the particle distribution and in which these particles will be combined to form larger agglomerates, in which the original initial particle can still be identified [20], [21] Agglomeration techniques can be broadly classified into two categories depending on whether the process is performed dry (by pressing technology, extrusion, etc.) or wet, in the presence of a granulation binder [22]. Since wet granulation is the method used in this paper, only wet granulation is discussed in detail, this is achieved by wetting with a binder and mixing the solid particles in a moving vessel, or a fluidized air bed, or a high shear mixer or other similar equipment. Regardless of the technology used, the granulation binder will be dispersed by contact and transfer in a mechanically created shear field [23]. The binder will thus contribute to the association of the particles with each other through a combination of capillary and viscous forces until a permanent bond is formed during the drying of the product by cementation or gelatinization, or by a chemical reaction with the solid substrate [24], [25].

Wet granulation can be considered as a combination of three rate processes as defined by Iveson et al [24], : wetting and nucleation when the binder is distributed throughout the powder mass forming initial nuclei, consolidation and growth when collisions between granules as well as between granules and initial powder particles result in increased compaction and granule size, and attrition and breakage when granules deform or break under the action of shear and impact forces. Several processing conditions of high-intensity granulators play critical roles on the characteristics of fabricated granulates [23], [26]–[34] , such as operation speeds of the impeller and/or container, granulation time, chopper speed, etc.,

Carbonation is considered the most common chemical reaction that influences the performance of materials in the environment. The void spaces within the hydrated material fill up with water first. When the material dries in the open air, it becomes depleted of water and air partially fills the pores. Carbon dioxide present in the atmosphere can then diffuse through the gas phase into the pores of the

material and dissolve into the pore solution. As the reactions (1), (2): the dissolved CO_2 passes from the form H_2CO_3 (carbonic acid) to HCO_3^- (bicarbonate ion) then to CO_3^{2-} (carbonate ion) which is the most abundant form when the pH is between 10 and 14. Indeed, when a solution is exposed to atmospheric CO_2, the gas dissolves and absorbs water in the form of carbonic acid (H_2CO_3) [35], [36]:

$$CO_{2(g)} + H_2O_{(aq)} \longleftrightarrow H_2CO_{3(aq)} \quad (1)$$

$$H_2CO_{3(aq)} \longleftrightarrow 2H^{2+}_{(aq)} + CO_3^{2-}{}_{(aq)} \quad (2)$$

Fresh WPFA contains reactive alkaline constituents (mainly $CaO/Ca(OH)_2$) and exhibits a high leachability of MMTE (e.g. Ba, Pb) [37]. The carbonation reduces the mobility of the aforementioned MMTE in WPFA according to the reaction (3):

$$M^{2+}_{(aq)} + CO_3^{2-}{}_{(aq)} \longleftrightarrow MCO_{3(s)} \quad (3)$$

Carbonation has many advantages such as the agglomeration of particles to form solid aggregates (the hardening of the matrix allows to obtain resistant finished materials) and the physical (pollutants) and chemical (formation of insoluble metal carbonates and pH decrease) stabilization. For all these reasons, the valorization of WPFA (rich in CaO) is particularly adapted to the carbonation process.

In order to develop the field of valorization of building materials based on WPFA within the sector of the Building and Public Works, it is necessary to carry out a methodology of characterization of the intrinsic properties of these by-products (the carbonated aggregates). For these purposes, the study of morphological, physical, chemical, mechanical and thermal characteristics of these aggregates is presented. In this perspective, the LWA manufacturing process and the influence of the granulation parameters on the granule properties will be mainly presented, then, in a second part, the process of accelerated carbonation of the manufactured aggregates. Finally, the aspects to evaluate fabricated granulates before and after carbonation include the particle size distribution, granule class, apparent density, actual density, organic matter content, leaching characteristics, % chloride (Cl), sulfates soluble in acid, % total sulfur, compressive strength, crushed particles, porosity, water adsorption and thermal conductivity were realized according to the standard EN 13055-1[38].

159 ## 2. Materials and methods

160 ### 2.1. Waste Paper Fly Ash used in lightweight aggregate production

161 The WPFA used in this study was collected from the cyclone of a mass-burning incinerator located in
162 the North-East of France. The ash type used in this paper were biomass and waste paper sludge ash.
163 The chemical composition was determined by X-Ray Fluorescence (XRF) and leaching of metallic
164 and metalloids trace elements (MMTE) from the WPFA was confirmed by Inductively Coupled
165 Plasma-Optical Emission Spectrometry (ICP-AES), the results are shown in **Table 1**. The chemical
166 composition of WPFA is as follows: CaO 64.02 %; SiO_2 14.59 % and Al_2O_3 8.1 %. The results
167 revealed that the concentration of Pb 7.35±0.6 mg/kg, Ba 178±6 mg/kg and Cl 1422±72 mg/kg were
168 the most abundant trace elements in the WPFA. The leaching of Ba, Pb and Cl from the WPFA
169 exceeded the limit values for landfill (Inert: 0.5 mg/kg, 20 mg/kg and 800 mg/kg for Ba, Pb and Cl
170 respectively) [39] and should be considered. The concentrations of copper (Cu), molybdenum (Mo)
171 and zinc (Zn) in the WPFA are relatively low.

172 **Table 1.** Chemical composition in major and MMTE of the WPFA.

173 The physical and chemical properties of WPFA were determined through various characterization
174 tests. Brunauer Emmett–Teller (BET) method was used to determine the specific surface area of the
175 WPFA from nitrogen sorption experiments using an AGITENT Analyzer apparatus from
176 Micromeritics in accordance with standard NF EN ISO-18757 [40], Physical adsorption results from
177 relatively low forces (Van der Waals forces) between the gas molecules (adsorbate) and the sample
178 surface (adsorbent). 1.5 g of dry sample was weighed and placed in the cell. The entire measuring cell
179 was immersed in a nitrogen bath to maintain a constant temperature. Successive quantities of nitrogen
180 were then introduced into the cell containing the sample, which had been degassed for 8 hours at
181 80°C. The adsorption/desorption isotherms were measured on the previously desorbed samples at
182 80°C, 5 mbar. The residual pressure is used to calculate the specific surface area, which is directly
183 related to the quantity of nitrogen adsorbed. The BET method used on WPFA allows reliable surface
184 measurements (<10% error).".

185 The specific density was measured using a Micromeritics ACCUPYC 1330 Helium Pycnometer in
186 accordance with standard NF EN 1097-7 [41]. Three samples were prepared in order to promote
187 consistency of results. The samples were dried at 105 °C to constant mass. Finally, a mass of
188 approximately 1.5 g of sample was weighed and placed in a cell with a total volume of 3.5 cm3. The
189 pycnometer performed several measurements on the same sample and the average of the
190 measurements was recorded.

191 Particle size distribution was determined with laser diffraction Coulter LS12330 in accordance with
192 standard NF EN ISO 13320-1[42]. This instrument is used to determine the size of particles between
193 0.04 µm and 2000 µm. Following the granulation process, particle size analysis is performed to
194 determine the particle size distribution of the manufactured aggregates. The test was carried out in
195 accordance with the European standard NF EN 933-1 [43]. The particle size analysis was carried out
196 by the dry method, using the sieves recommended by the European standard NF EN 933-2 [44]. The
197 test represents the reference test for measuring the granulometry of aggregates. The sieves used are: 2,
198 4, 8, and 16 mm. Each sieve is weighed empty and then full in order to verify that the mass of each
199 reject is less than the saturation mass of the sieve. The test is carried out 3 times for each lot of
200 aggregate.

201 The conductivity and pH were determined use batch leaching tests made according to the standard NF
202 EN 12457-2 [45]. **Table 2** illustrates the results of the physical-chemical characterization of WPFA.

203 **Table 2.** Physical and chemical characterizations of WPFA

204 The WPFA used in this study conforms to the requirements of Class C as specified by ASTM C 618
205 (Class-C) [46] which is shown in **Table 3**.

206 **Table 3.** Chemical properties of WPFA and specification requirements.

207 Particle size distributions of the WPFA used in LWA production are illustrated in **Fig.1**. It can be seen
208 that the WPFA has a fine particle size distribution (< 250µm) and 50% of particles smaller than 10µm.

209 **Fig. 1.** Granular distributions of WPFA.

2.2 Granulation process

The WPFA granules are fabricated in a 5L Eirich high-intensity granulator (Eirich R-02) manufactured in Hardheim, Germany. Impeller, chopper and steel pan (container) are important components of this machine, as shown in **Fig. 2**. The chopper is a static tool which prevents deposit build-up on the vessel wall. The steel pan and the impeller can be operated in the counter-current and co-current flow modes. The impeller inside can rotate both at clockwise and anti-clockwise directions, while the steel pan (positioned horizontally) can only rotate in a clockwise direction. Thus, two different rotation modes can be generated when we combine the rotation directions of impeller and the steel pan in different ways: cross current rotation mode, where the pan rotate clockwise but the impeller rotate anti clockwise; counter current rotation mode, where both the pan and the impeller rotate clockwise.

Fig.2. Eirich high-intensity granulator

The rotation speed of impeller has been kept constant: 3000 rpm for the period of nucleation formation and for the period of granulate growth, in order to study the effect of steel pan rotation speeds (85 rpm and 170 rpm). The granulation procedure employed in this study is as follows:

- Dry WPFA was weighed (1000g), homogenized and added to the steel pan.
- After switching on the steel pan and the impeller, 300 g of tap water was sprayed via wash bottle on the WPFA. The time to add tap water is 90 second. Within this period of time, secondary units of nuclei come into birth, and we thus name it as the nucleation time.

Sprayed water was used as an agglomeration binder and coagulation so that the wet mixture (WPFA rich in CaO + water) was hydrated and transformed into LWA by the rolling motion and the effects of capillary attraction by an inclined turntable. During the granulation process, granulate starts to grow, and a period of 3 min was set as the granulating time. it is necessary to specify, surplus water caused bigger and irregular particles and insufficient water led to difficulty in granulation, as also confirmed by Chiou et al, [47]. To investigate the effect of granulation time and flow patterns within the steel pan on the properties of generated granulation, we varied the impeller rotates differently: counter current flow, cross current flow, then, the granulation time from 3 min to 9 min. After the granulation process,

236 the granulates within the range between 2 and 16 mm were selected by the sieving process, then, each
237 batch of LWA was sealed in air-tight plastic bags and stored at room temperature before were
238 carbonated. The different granulation parameters are outlined in **Table 4**.

239 **Table 4**. The different granulation parameters of the WPFA.

240 **2.3 Lightweight aggregate carbonation process**

241 Carbonation has many advantages such as hardening of the matrix to obtain resistant finished LWA,
242 physical stabilization (of pollutants) and chemical stabilization (formation of insoluble metal
243 carbonates $BaCO_3$/$PbCO_3$ and decrease of pH). To this observation, an accelerated carbonation
244 process was developed allowing the reaction of $Ca(OH)_2$ portlandite/calcium oxide (CaO) as well as
245 Ba and Pb from LWA with CO_2**.**

246 The CO_2 is transformed into carbonic acid which can then initiate reactions with calcium hydroxide
247 compounds (portlandite or lime) to form calcium carbonates. The precipitation of carbonates (Calcite)
248 causes the permanent fixation of CO_2.This process aims to carbonate LWA in an atmosphere enriched
249 in carbon dioxide in order to generate inert aggregates. The manufactured LWA were treated with
250 carbon dioxide (CO_2) in a pressure reaction vessel (see **Fig. 3**).

251 **Fig.3** LWA carbonation apparatus

252 The LWA were mixed with sufficient tap water (ratio of liquid to solid of 0.3 l/kg) and then
253 carbonated in a 100% carbon dioxide atmosphere held at 0.5 bar pressure for 72 h. Saturated sodium
254 chloride solution maintained the relative humidity at 65% inside the reaction vessel. Maintaining
255 humidity around this level is for efficient carbonation [48].

256 Analysis of LWA shape and morphology before and after carbonation was performed at high
257 magnification using electron microscope (SEM- Hitachi S-4300SE/N), energy dispersive spectroscopy
258 (EDS) observations and the Zeiss digital microscope.

259 **2.4 Lightweight aggregate characterization**

The characteristics of the manufactured LWA have a very important role on the properties and performances of concrete or mortar (injection mortar). In fact, the properties of concrete are largely influenced by the characteristics of its constituents. For this reason, in order to develop the field of the valorization of the LWA based on WPFA, we proceeded out tests of characterization of these LWA before and after carbonation, according to the standard EN 13055-1[38]. Then we compared these characteristics with commercialized LWA from ARGEX.

The bulk densities ρ_{app} of the LWA were measured according to NF EN 1097-3 [49] with a 1-liter container. The helium pycnometer method, in accordance with NF EN 1097-6, was used to obtain the absolute densities of the LWA. We determine the densities in order to verify the mineralogical regularity of the materials.

The porosity measurement of LWA was performed according to the NF P94-410-3 [50] standard, with a MicroActive AutoPore V 9600 2.00 mercury porosimeter.

The measurement of water absorption of LWA was made on three samples of 500g immersed in water for 24 hours in order to measure the capacity of a LWA to absorb water according to the standard NF EN 1097-6 [51]. This test is performed in order to consider the absorption of aggregates in the calculation of the water/cement ratio in concrete and to have an estimate of the ability of the LWA to influence the rheology of the concrete.

In order to evaluate the mechanical strength of LWA, bulk crushing tests were performed according to EN 13055-1 [38]. A sample of LWA compacted by vibration is compressed, with the help of a piston, in a cylinder of 100 mm height and 175 to 200 cm² of section. The speed of the plunger is 1 mm per minute and the test is completed when the plunger has reached 20 mm. The conventional strength of the LWA is defined as the quotient of the applied force required to achieve 20 mm of piston depression per cylinder cross-section.

The percentage of chloride, sulphate soluble in acid, total sulfur and the loss on ignition were determined according to standard NF EN 1744-1 [52]. The three methods of measuring the solubility

of chloride, sulphate soluble in acid, total sulfur is determined gravimetrically, the sulphate content is expressed as a percentage of Sulphur trioxide per mass of LWA (% SO_3).

To measure the thermal conductivity of LWA, we used the steady-state hot plate method on 25x25x6 cm samples. The material sample to be studied is placed between two plates, hot and cold, and surrounded by insulation to avoid lateral losses of heat flow. Thermocouples are installed on the faces of the sample to measure the temperature differences. The upper plate hot is lowered until it is in contact with the material and the acquisition is launched.

3. Results and discussion

3.1 Effect of rotation speed of the steel pan

According to Iveson's theory of the granule formation process [27], granules form in two continuous stages, wetting/nucleus formation and the growth period. Apparently, a faster rotation speed of the plate creates more chances for solid powders to contact the sprayed liquid droplets; thus, a larger quantity of small nuclei can be formed. In the case of a low rotation speed, the liquid droplets can remain on the surface of the solid powders for a relatively longer period of time, which reduces the chances of the solid powders meeting the liquid droplets. During the next period of granule growth, these previously formed nuclei will have different ways of "growing" themselves: by attaching to other pre-formed nuclei (nuclei agglomeration) or by attracting free powder to their surface (powder attachment) [53]. In the case of a high rotation speed, more nuclei have been generated, and thus, these preformed nuclei are more likely to encounter each other (nuclei to nuclei attachment), and their growth tends to follow a nuclei agglomeration path; in the other case, the number of nuclei is limited, and thus, they are more likely to encounter fine powders [53].

Fig 4 show size distribution for LWA fabricated under counter current rotation mode. Maintaining a constant rotation speed of impeller (3000 rpm) and rotation mode between the impeller and the steel pan (counter current rotation mode), we have produced LWA under two different rotation speeds of the steel pan (85 rpm and 170 rpm). The variation of rotation speeds of the steel pan has brought a difference to the growth rate, which has been proved by the investigation of the LWA size distribution

311 **(Fig. 4)**. Clearly, faster rotational speed shifts the size of the granules to larger values, indicating that
312 the rate of increase in granule size is faster when they develop from agglomeration of the nuclei than
313 from the attachment of the fine powder to the nuclei. In addition, it can be seen that a higher rotational
314 speed (170 rpm) generates a higher yield of larger granules, while a lower rotational speed (85rpm)
315 favors the creation of a greater amount of smaller granules [53]. This will apparently vary the final
316 granulates yield within a certain size range, which is interesting information for people who want to
317 improve the granulates yield with certain sizes.

318 **Fig.4** Size distribution for LWA fabricated under counter current rotation mode

319 **3.2. Effect of rotation modes**

320 Two different rotation modes are available in the Eirich high-intensity granulator, they differentiate
321 each other from the rotation directions of the impeller: cross current rotation and counter current
322 rotation. When the machine operates in cross current rotation mode, powders are taking up the whole
323 space and distribute homogeneously within the steel pan. While in the case of counter current rotation
324 mode (both the impeller and the steel pan rotate in clockwise directions), due to gravity reason,
325 powders tend to 'concentrate' more in the lower part of the steel pan [53].

326 **Fig 5** shows the size distribution of LWA fabricated under these two different rotation modes. **Fig 5**
327 shows that despite the pan rotation speed differences (85 rpm and 170 rpm), granulates are larger from
328 cross current rotation mode than from counter current rotation mode. This information also indicates
329 that there are fewer powders in the upper part of the pan (where the liquid was added) for the counter-
330 current rotation mode than for the cross-rotation mode; thus, fewer nuclei will be formed for the
331 counter-current rotation mode, and the granules will grow in a way of powder attachment. Conversely,
332 more nuclei will be formed in the cross-rotation mode, and the granulate will grow in a way of nuclei
333 agglomeration mode. In other words, the generated granules are larger when the initial powders are
334 homogeneously dispersed in the steel pan rather than relatively "concentrated" in the lower part of the
335 steel pan. Since powder dispersion directly affects the chances of powders coming into contact with
336 other powders, we can say that the better dispersion created by the cross-flow rotation mode creates

more chances for cores to encounter other cores or loose powders (rapid incorporation), which is beneficial for a faster growth rate of the granules, and vice versa [53].

Fig.5 Size distribution of LWA fabricated under different rotation modes

3.3. Effect of granulation time

The rotation modes between impeller and steel pan and both the steel pan rotation speed affect the growing behavior of LWA, with the steel pan rotation speed controlled at 170 rpm and the rotation mode in cross current throughout (95% of LWA have a grain size between 2 and 16 mm), the size distribution of the LWA made under these conditions under different granulation time (3, 6 and 9 min) is shown in **Fig. 6.**

Increasing the granulation time from 3, 6 to 9 min improved the yield of the LWA with the size range <4 mm (from 22.2 wt% to 95.5 wt%). However, increasing the granulation time to 9min resulted in a decrease of targeted LWA yield to 80 wt% by forming more larger LWA within the size range of 4mm to <1 mm.

The amount of LWA less than 1 mm is increasing from 1.9% to 6%, while the ratios of larger LWA (8-16mm) are decreasing continuously. However, the size changes between 3 to 6 min are relatively smaller, whose relative mass ratio differences are between 1.1 and 1.8. The changes from 6 to 9 min are much larger, whose mass ratios rise to more than 10 times the difference in the case of LWA < 4mm. Inversely to the trend observed in the study of the steel pan speed, the increase of granulation time resulted in the formation of smaller LWA, which was clearly shown in the diameters of the manufactured LWA in **fig.6**.

Fig. 6. Effect of the granulation time on the size distribution of LWA produced.

This is attributed to the hydraulic properties of the lime present in the WPFA which hardens rapidly by mixing with water during the first 3 minutes of granulation. Apparently, with the increase of the granulation time (6 to 9 min), the LWA of diameters higher than 4mm, undergo physical interactions on the one side with the turbine and on the other side with the other LWA, which results in the reduction of their sizes.

This information does not agree with the results reported in the research work done by Mangwandi et al., [30] in which the authors indicated that a longer granulation time could help consolidate the microstructure of the LWA formed. In contrast, Walker et al. showed that as the granulation time of lactose increased, an increase in mean particle size had been found [54].

3.3. Effect of carbonation

To investigate the effects of carbonation on the leachability, mechanical strength and the porous properties of the fabricated LWA, we have performed accelerated carbonation on the fabricated LWA under the following conditions: Cross-current/ 175 rpm / 3 min (95% of the manufactured LWA have average size distributions vary from 16 mm to 2mm).

3.1.1 Thermogravimetric analysis (TGA):

Fig 7 shows the thermal characteristics of the WPFA and the LWA before and after carbonation. The WPFA and the LWA before and after carbonation present a mass loss between 90 °C and 300 °C corresponds to the deshydroxylation of hydrates including ettringites and carboaluminates [55]. The mass losses corresponding to carboaluminates appeared in the case of carbonated LWA and non-carbonated LWA, and ettringite in the case of carbonated LWA, which confirms the hydraulic properties of our WPFA, since both portlandite participates in the hydration reaction and the carbonation reaction during the 3 days of the accelerated carbonation.

However, the mass loss observed between 400 °C and 500 °C corresponds to the deshydroxylation of Portlandite [56], the intensity and peak broadening in the case of carbonated LWA decreased compared to the WPFA. It is important to note that mass loss between 550 °C and 950 °C corresponds to the decarbonation of the calcites. This peak is more important in the carbonated LWA which is normal considering the carbonation process (100% CO_2). Confirming that lime and portlandite which represent major phases in the WPFA were transformed through carbonation to calcite.

In the study done by Dijkstra [55], the carbonation of both ashes was studied. During the carbonation, the quantity of reactive aluminates (mayenite) decreased by transformation into ettringite and

carboaluminate [55], which reduces the risks of expansion since the expansive phases (ettringite, carboaluminate) are formed before the incorporation of LWA into concrete.

Fig 7. The thermal characteristics of the WPFA and LWA before and after carbonation

3.3.2 Microstructure evolution before and after carbonation

The surfaces of the LWA were used to determine the microstructure by using the Zeiss digital microscope **(Fig.8 a, b, c, d)** and scanning electron microscope (SEM-EDS) (**Fig.8 e, f).**

Morphological analysis revealed structural differences between carbonate and non-carbonate LWA. The non-carbonated LWA have an explicit porous structure in the middle of a granule while their surface layers are denser **(Fig.8 a, c)**. The black dots in the image are pores, which were most probably produced by the enclosure of air bubbles in the granulation procedure. The structure is very dense in general. **Fig (9a)** shows another SEM image with higher magnification than **Fig (8c)**. In this image also, it can be seen that the structure is very dense, A crack is also clearly visible in the figure, probably resulting from the splitting of the granule, thus, a significant porosity.

After carbonation **(Fig 8 b, d)**, as can be seen, the LWA have a clearly denser structure than the non-carbonated LWA structure. In addition, the surface is more irregular, indicating that precipitation may have formed during the carbonation process. The change in color and disappearance of pores after carbonation of the LWA may also be the result of the reaction between $Ca(OH)_2$ and carbon dioxide, eventually forming calcite between the particles and filling the pores.

Fig.8. Optical images of the LWA made by from WPFA before **(a,c)** and after **(b,d)** carbonation (Zeiss digital microscope)

Fig 9 (a and b) shows a SEM image of the carbonated LWA before and after carbonation. At this level, it is possible to see a new layer that has precipitated on the surface that is probably calcite, as well as solid bridges between the precipitates, which bonds them together. The precipitation of calcite is the most probable binding mechanism due to the reaction between CaO and water as was mentioned in the literature review.

Only a few scientific studies can be found concerning the study of the inner and outer porosity/density of the LWA; similar results in relation to our date are mentioned, but not completely investigated by other scientists [57], [58]. The authors observed that the porosity/density of the particles tended to decrease, which probably occurred due to the fact that the densification, consolidation and compaction of the particles increased with increasing granulation time. The others concluded that the densification process reduced the porosity of the granules and induced the migration of the binder to the surface of the granules. Thus, saturation was achieved due to the reduction of pore space by consolidation rather than due to pore filling promoted by the addition of binder."

SEM observations of the carbonated LWA show that the majority of the grains on the LWA have irregular shapes (Fig 9 c and d) with the presence of a few spheres (Fig 9 c). On the other side, the carbonated LWA have a less porous structure compared to the non-carbonated LWA. Importantly, ettringite is present in the form of needles about 10 microns long (Fig 9 d). EDS observations of the carbonated LWA similarly confirm the presence of calcite (Fig 9 e), and ettringite (Fig 9 f). Consistent with the TGA results confirming the formation of hydrates including ettringite/ carboaluminate (90-300 °C) and calcite (550-950 °C) in the carbonated LWA. Several authors have suggested the formation of ettringite ($Ca_6Al_2(SO_4)_3(OH)_{12}$. $26H_2O$) when WPFA is hydrated due to the presence of mayenite ($Ca_{12}Al_{14}O_{33}$), anhydrite ($CaSO_4$) and free lime (CaO) [55], [59].

Fig.9. SEM-EDS picture of the LWA before **(a)** and after **(b)**, **(c)**, (**d), (e), (f)** carbonation

3.3.3 Influence of carbonation on leaching

Many studies have demonstrated that when LWA undergo carbonation, the immobilization of MMTE (such as Ba, Pb, Zn) is generally enhanced, minimizing the leachability of these elements [60], [61]. **Table 5** lists the concentrations of MMTE leached from WPFA, carbonated LWA and the legal limits (IWSI) for the use of LWA based on WPFA in civil engineering in France.

Since the chemical composition results (Table 5) showed that the WPFA had high amounts of Ba and Pb, an analysis of the concentration of these trace metal elements as well as other elements was

performed on the eluates extracted from the leaching test performed on the carbonated LWA sample after crushing, according to standard 12457-2.

The results displayed in Table 5 on the concentration of the MMTE eluate concentration in the WPFA corroborate that there is a predominance of Ba (178±6 mg/kg) and Pb (7.35±0.6 mg/kg) compared to the rest of the elements measured (Cu=0.09±0.02 mg/kg, Mo=0.08±0.02 mg/kg, Zn=1.1±0.2 mg/kg while As, Cr, Sb, and Se were not detected). When these results are compared to the leaching of carbonated LWA, it can be observed that carbonation seems to have favored a decrease in the leachability of certain elements, in particularly Zn <0.01 mg/ kg, Pb<0.03 mg/kg and especially Ba=0.3± 0.05 mg/kg. The leachability of Ba and Pb is 99% lower in the carbonated LWA than in the original WPFA, demonstrating that carbonation has played an important role in the immobilization of this element. It was also found that the leaching of calcium followed the same trend as Ba and Pb, the leaching is reduced after carbonation (from 10 839±521 mg/kg to 451±7 mg/kg) which confirms that the majority of calcium was carbonated. The calcium leaching is presented in Supplementary data (Table 1). The formation of $BaCO_3$, $PbCO_3$ and $ZnCO_3$, an insoluble barium, lead and zinc carbonate compounds, has been considered as the immobilization mechanism of Ba, Zn and Pb [62]. In addition, a few studies have reported the immobilization of Ba and Zn in type F FA with carbonation [58], [59]. In a previous study [63], accelerated carbonation (100% CO_2) decreased the leaching of Pb and Zn by forming insoluble compounds such as $PbCO_3$ and $ZnCO_3$ which is consistent with what we assumed [62].

The leachability of sulfate and fluoride were below the legal leaching limit (IWSI) before and after carbonation. The chloride concentration exceeded the IWSI threshold even after carbonation, which indicates that the carbonation process has no influence on the immobilization of salts.

In general, cationic species immobilize well after accelerated carbonation. This behavior has been explained by the precipitation of elements as carbonates, since in a high pH environment, elements such as Ba and Pb would be hydroxic, they would not be able to precipitate as hydroxides. In this study, the original pH of the WPFA was 13.5, whereas that of the carbonated LWA showed a lower pH = 10.39 after only 3 days of carbonation, as a result of the rapid consumption of calcium hydroxide

466 ($Ca(OH)_2$) during the carbonation process and the formation of calcite ($CaCO_3$). This result clearly
467 demonstrates that the decrease in pH explains the behavior of Ba and Pb after carbonation. It also
468 justifies the theory that pH decrease by carbonation is the dominant mode of stabilization [62].

469 In order to determine if the concentrations of these MMTE could be harmful to the environment, the
470 results have been compared to the IWSI limits. As can be seen **(Table 5)**, Ba and Pb are well below
471 the maximum permitted values. This means that the eluates of these LWA do not represent a real
472 threat to the environment, but on the contrary, they can be used safely from an environmental point of
473 view.

474 **Table 5.** Concentration (mg/kg) of MMTE in WPA and Carbonated LWA

475 **4. Lightweight aggregates characterization**

476 **4.1 Absolute density, bulk density and apparent density**

477 The absolute density, bulk density and apparent density are important factors when LWA properties
478 are considered [64]–[66], the bulk density of common artificial LWA is generally between 300 kg/m^3
479 and 1300 kg/m^3, which is two to three times less than that of common aggregates. The results of the
480 LWA are shown in **Table 6**. The various characterization methods have shown that the aggregates
481 manufactured from the ash can be classified as LWA, as all fall within the set limits of loose bulk
482 density (≤1.20 kg/m^3) and particle density ≤2.00 Mg/m^3 (BS EN 13055-1).

483 The Absolute density results of carbonated and non-carbonated LWA were found to be in the range of
484 2105-2370 kg/m^3 respectively. The carbonated LWA was found to be denser than the non-carbonated
485 LWA and their density values are higher than the aggregates commercialized by Argex (550 kg/m^3),
486 Similar trends in results were found for bulk density and apparent density. The enhancement in the
487 density was due to $Ca(OH)_2$ from the WPFA reacting with CO_2 to produce a solid volume of Calcite
488 ($CaCO_3$), leading to a reduction in porosity throughout the carbonation. In addition, $CaCO_3$ also
489 improved the density of LWA due to its high density (2.71kg/m^3) as compared to $Ca(OH)_2$ (2.24
490 kg/m^3).

491 **Table 6.** Characterization of LWA according to the standard (NF EN 13055-1)

492 **4.2 Porosity and water Absorption**

493 Carbonated LWA have a lower porosity (21%) than non-carbonated LWA (29%). As the porosity
494 decreases with carbonation time, the water absorption coefficient at 24 h decreases. Based on
495 experimental results, a relationship between water adsorption and porosity was found, the higher the
496 porosity, the more water is adsorbed.

497 As shown in **Table 6**, an absorption of 27.9% was measured for non-carbonated LWA. After 3 days of
498 carbonation, the LWA reached about 21% water absorption. Overall, the manufactured LWA either
499 before or after carbonation was comparable to the Argex aggregate in terms of porosity and density,
500 although it had lower water absorption. Carbonation of the aggregates for 3 days resulted in a decrease
501 in porosity, this confirmed what we obtained in the SEM images, a layer of calcite was formed and
502 thus filling the pores.

503 The high porosity of LWA presents a problem when mixing them to produce concrete or mortar.
504 Therefore, when using these eco-aggregates to formulate concrete or mortar, it is necessary to consider
505 the water absorption by the aggregates. Lower porosity leads to lower water absorption. These results
506 for water absorption agree with the results for density in which water absorption decreases with
507 increasing density.

508 **4.3 Compressive strength**

509 The compressive strength of LWA is an important factor in concrete, as LWA are the weakest
510 component of concrete [67]. Non-carbonated LWA have a lower bulk crushing strength (3.15MPa)
511 than ARGEX aggregates (4.7MPa), as expected from the composition as well as the bulk and absolute
512 density. The carbonated LWA tend to show higher mechanical performances superior (7.6 MPa) to the
513 Non-carbonated LWA and the Argex aggregates. These results reflect the interest of carbonated
514 aggregates in the field of civil engineering.

515 The effect of carbonation is very significant in type C of FA, this is due to the large amount of reactive
516 CaO in WPFA, which reacts with water to form ($Ca(OH)_2$), the fact that the slaked lime containing
517 aggregates were found to be resistant, and that exposure to 100% CO_2 promoted the development of

518 resistance, indicates that the carbonation step is well optimized further to form $CaCO_3$ bridges. The
519 strength increases significantly after carbonation, this confirms what we observed in SEM and TGA
520 imaging, $Ca(OH)_2$ reacts with CO_2 forming solid calcite bridges in the particles which improves the
521 compressive strength of the granules.

522 In a study by Bui et al [68], the compressive strength of alkali-activated aggregates prepared from rice
523 husk FA, blast furnace slag, and class F FA varied from 5.5 to 14.5 MPa. Gonzal et al [65], [66], [69],
524 [70] have used several different precursors, such as FA, washing aggregate sludge, used motor oil,
525 mining and industrial waste, then the aggregates are prepared by sintering in a rotary kiln. The bulk
526 compressive strength of the aggregates is between 2 and 14 MPa.

527 Several studies have shown that the manufacture of artificial aggregates by granulating various wastes
528 as raw materials with cement, leads to strengths between 1 and 7 MPa. Surprisingly, despite the
529 different precursors and preparation methods used, the strength values are so similar to those
530 previously studied. Ferrone et al., [71] has previously reported that commercial lightweight expanded
531 clay aggregates (Leca) have compressive strengths varying from 0.7 to 4.5 MPa, depending on the
532 size. This confirmed that LWA made from WPFA before and after carbonation have equivalent
533 mechanical performance compared to aggregates made in other studies, also for commercial
534 aggregates widely used (Argex) and can therefore replace them in civil engineering applications.

535 **4.3 Thermal conductivity**

536 The results presented in Table 6 show excellent thermal performances for the LWA before and after
537 carbonation with a thermal conductivity of 0.19W/m.°C and 0.32W/m.°C respectively, similar to that
538 of the Argex aggregate (0.14 W/m.°C).

539 The absolute density of LWA before carbonation was 2105 kg/m3, thus the porosity was higher (29%)
540 which explains the high thermal performance of non-carbonated LWA. After carbonation, the porosity
541 decreases (19.8%), because of the $CaCO_3$ formed at the surface and the absolute density value
542 increases (2370 kg/m^3), this increase in density and the decrease in porosity led to a significant
543 decrease in the insulating capacity of the aggregates. If the thermal conductivity of the aggregates

544 depended only on their total porosity or on the density of the aggregates, the conductivity/density
545 ratios of the different aggregates would be similar regardless of the nature of the aggregate.

546 This was also illustrated by Nguyen [72] in his studies on the characterization of insulating LWA; an
547 order of magnitude conductivity of 0.4 W/m.°C was achieved. The author also presents the hypothesis
548 that the denser external surface of the expanded shale aggregates can constitute a "thermal bridge"
549 favoring the transfer of heat and thus lead to a slightly higher thermal conductivity of the aggregate,
550 which is consistent with the results of this paper. According to Valore [73], the thermal conductivity of
551 LWA depends mainly on its absolute density; thus, its honeycomb structure confers an interesting
552 thermal conductivity and thermal expansion. As an example, the classic aggregate has a thermal
553 conductivity of 1.75 W/m.°C while that of the LWA of expanded clay or expanded shale is between
554 0.10 and 0.80 W/m.°C [74]. This gives the LWA a higher thermal insulation. In addition, LWA has a
555 high degree of fire resistance due to its low thermal conductivity and low coefficient of thermal
556 expansion [75]. Fire resistance is not discussed in this study.

557 **4.4 Loss on Ignition**

558 According to Table 6, the loss on ignition value of LWA before and after carbonation is 27.2% and
559 31.3% at 900°C, respectively. At the same time, the loss on ignition at 900°C was measured to explore
560 the thermal instability of LWA before and after carbonation. It should be mentioned that the total mass
561 loss observed in the loss on ignition only reflects the contribution of the residual organic matter. The
562 mass loss from 0 to 550°C due to the loss of bound water, organic matter and clays, between 350 and
563 550°C corresponds to the deshydroxylation of portlandite, and when the temperature is higher than
564 550°C up to 900°C the mass loss corresponds well to the decarbonation of the different modes of
565 calcium carbonates (aragonite, vaterite, calcite).

566 Based on the loss on ignition and TGA results, the percentage of organic matter in LWA before and
567 after carbonation can be estimated using the following relationship:

568 **% Organic matter = Total mass loss – (% CSH deshydroxylation mass + % $Ca(OH)_2$**
569 **deshydroxylation mass + % $CaCO_3$ decarbonation mass)**

570 The difference in mass loss at 900°C of LWA due to hydrate formation, lime hydration and carbonate
571 formation as we observed in the TGA. The percentage of organic matter seems to be similar before
572 and after carbonation (5.76% before carbonation and 5.08% after carbonation), which shows that
573 carbonation has no influence on organic matter.

574 **4.5 Solubility tests: acid-soluble sulphates and acid-soluble sulphates**

575 The determination of the chemical and mineralogical composition in the LWA should be concentrated
576 on the determination of % total sulfur, % chloride and % acid soluble sulfates. The percentages
577 determined for chloride, total sulphur and acid soluble sulphates of the LWA before and after
578 carbonation were similar (Table 6).

579 The content of acid soluble sulfates and chloride ions defines a designation of aggregates without a
580 threshold being imposed. However, a maximum value of 0.01% and 0.8% respectively for the content
581 of chloride ions and acid soluble sulfate are recommended [66].

582 In fact, a too high sulfate content leads to a risk of secondary ettringite formation or Candlot salt. The
583 presence of chloride in LWA can cause premature corrosion in concrete or mortar after migration of
584 ions. A high presence of chloride can also cause the formation of lime chloroaluminate or Friedel salt,
585 which is expansive. It is determined according to the EN 1744-1 standard (Afnor, Norme NF EN
586 1744-1). Degradations can occur in concrete formulated with aggregates with a high sulfide content,
587 sulfides can be transformed into sulfates by oxidation. The sulfates in turn can influence the setting
588 and cause swelling (secondary ettringite) and thus lead to an increase in the porosity of concrete. This
589 porosity can then have an important role in case of attack of the concrete by external agents such as
590 sulphate or chloride solutions. Their presence is related to the operating environment of the structure,
591 and a higher porosity facilitates the penetration of these aggressive elements towards the core of the
592 materials and by increasing the reaction surfaces [66]. For this reason, carbonation was necessary to
593 decrease the percentage of porosity. In fact, the contents of LWA are not very high and are clearly
594 lower than those recommended by the standard.

595

5. Conclusion

This study shows the feasibility and optimization of granulation parameters, in order to fabricate LWA from WPFA (rich in CaO), by granulation with water in an Eirich high intensity granulator (Eirich R-02). An accelerated carbonation step was performed, exposing the manufactured LWA to pure carbon dioxide in order to evolve the immobilization potential of Ba and Pb, and to investigate the influence of carbonation on the physical, morphological, thermal and mechanical characterization of LWA.

- To adjusting the granulation parameters of the Eirich high intensity granulator to a constant impeller speed (3000rpm), the rotation speed of the steel pan (170 rpm), the rotation mode between the impeller and the steel pan in cross current and a granulation time of 3 minutes, 95% of the LWA were produced with the target size (2mm to 16mm).

- WPFA exhibited high reactivity to carbon dioxide. Accelerated carbonation of the LWA reduced the leaching of Ba and Pb with removal percentages exceeding 98% for both elements. TGA and SEM-EDS results confirm the formation of calcite after accelerated carbonation, as well as the formation of hydrates (ettringite and carboaluminates) due to the hydraulic properties of WPFA.

- The characteristics of LWA before and after carbonation are evaluated according to the NF EN 13055-1 standard in order to confirm the possibility of valorizing these eco-materials in the manufacture of concrete. These aggregates present a relatively low density, classifying them in the category of LWA. This weight reduction is due to the high porosity of these aggregates, suggesting a significant capacity of water imprisonment for the hydration of cement. Moreover, after carbonation the percentage of porosity and water absorption decreased, thus, the mechanical strength was improved (7.6 MPa). Finally, the measurement of the thermal conductivity of LWA is interesting and would lead to an improvement of the thermal performance of concrete

- However, in order to improve the valorization of these waste types, it is essential to improve the performance of the manufactured LWA. Many research perspectives are also envisaged to extend this study. These prospects may concern: (i) Testing other binders, allowing the improvement of the physic-chemical properties; (ii) Realizing sorption tests at different temperatures to evaluate the temperature influence on the hygric behavior of LWA; (iii) Substituting partially or totally ordinary aggregates by LWA in concrete; (iv) Studying the coupling between carbonated and non-carbonated LWA in concrete.

Acknowledgements

The authors wish to acknowledge technical contributions of the chemistry pole of Institut Mines-Télécom. This research did not receive any specific grant from funding agencies in the public, commercial, or not-for-profit sectors.

References

[1] S. Ray, A. K. Mishra, et A. S. Kalamdhad, « Hydraulic performance, consolidation characteristics and shear strength analysis of bentonites in the presence of fly-ash, sewage sludge and paper-mill leachates for landfill application », *Journal of Environmental Management*, vol. 302, p. 113977, janv. 2022, doi: 10.1016/j.jenvman.2021.113977.

[2] M. Cox, H. Nugteren, et M. Janssen-Jurkovičová, *Combustion residues: current, novel and renewable applications*. John Wiley & Sons, 2008.

[3] A. A. Tortosa Masiá, B. J. P. Buhre, R. P. Gupta, et T. F. Wall, « Characterising ash of biomass and waste », *Fuel Processing Technology*, vol. 88, n° 11, p. 1071-1081, déc. 2007, doi: 10.1016/j.fuproc.2007.06.011.

[4] D. Yao *et al.*, « Carbon footprint and water footprint analysis of generating synthetic natural gas from biomass », *Renewable Energy*, vol. 186, p. 780-789, mars 2022, doi: 10.1016/j.renene.2022.01.014.

[5] S. Wang, L. Baxter, et F. Fonseca, « Biomass fly ash in concrete: SEM, EDX and ESEM analysis », *Fuel*, vol. 87, n° 3, p. 372-379, mars 2008, doi: 10.1016/j.fuel.2007.05.024.

[6] R. Rajamma *et al.*, « Biomass fly ash effect on fresh and hardened state properties of cement based materials », *Composites Part B: Engineering*, vol. 77, p. 1-9, août 2015, doi: 10.1016/j.compositesb.2015.03.019.

[7] R. Rajamma, R. J. Ball, L. A. C. Tarelho, G. C. Allen, J. A. Labrincha, et V. M. Ferreira, « Characterisation and use of biomass fly ash in cement-based materials », *Journal of Hazardous Materials*, vol. 172, n° 2, p. 1049-1060, déc. 2009, doi: 10.1016/j.jhazmat.2009.07.109.

[8] T. C. Esteves, R. Rajamma, D. Soares, A. S. Silva, V. M. Ferreira, et J. A. Labrincha, « Use of biomass fly ash for mitigation of alkali-silica reaction of cement mortars », *Construction and Building Materials*, vol. 26, n° 1, p. 687-693, janv. 2012, doi: 10.1016/j.conbuildmat.2011.06.075.

[9] S. Ehsan, S. O. Prasher, et W. D. Marshall, « A Washing Procedure to Mobilize Mixed Contaminants from Soil », *Journal of Environmental Quality*, vol. 35, n° 6, p. 2146-2153, 2006, doi: 10.2134/jeq2005.0474.

[10] M. Isoyama et S.-I. Wada, « Remediation of Pb-contaminated soils by washing with hydrochloric acid and subsequent immobilization with calcite and allophanic soil », *Journal of Hazardous Materials*, vol. 143, n° 3, p. 636-642, mai 2007, doi: 10.1016/j.jhazmat.2007.01.008.
[11] A. Moutsatsou, M. Gregou, D. Matsas, et V. Protonotarios, « Washing as a remediation technology applicable in soils heavily polluted by mining–metallurgical activities », *Chemosphere*, vol. 63, n° 10, p. 1632-1640, juin 2006, doi: 10.1016/j.chemosphere.2005.10.015.
[12] C. N. Mulligan, R. N. Yong, et B. F. Gibbs, « Remediation technologies for metal-contaminated soils and groundwater: an evaluation », *Engineering Geology*, vol. 60, n° 1, p. 193-207, juin 2001, doi: 10.1016/S0013-7952(00)00101-0.
[13] H. Chen, C. Mangwandi, et D. Rooney, « Production of solid biofuel granules from drum granulation of bio-waste with silicate-based binders », *Powder Technology*, vol. 354, p. 231-239, sept. 2019, doi: 10.1016/j.powtec.2019.05.074.
[14] L. B. Andrade, J. C. Rocha, et M. Cheriaf, « Evaluation of concrete incorporating bottom ash as a natural aggregates replacement », *Waste Management*, vol. 27, n° 9, p. 1190-1199, janv. 2007, doi: 10.1016/j.wasman.2006.07.020.
[15] F. Liu, Y. Yan, L. Li, C. Lan, et G. Chen, « Performance of Recycled Plastic-Based Concrete », *Journal of Materials in Civil Engineering*, vol. 27, n° 2, p. A4014004, févr. 2015, doi: 10.1061/(ASCE)MT.1943-5533.0000989.
[16] N. U. Kockal et T. Ozturan, « Characteristics of lightweight fly ash aggregates produced with different binders and heat treatments », *Cement and Concrete Composites*, vol. 33, n° 1, p. 61-67, janv. 2011, doi: 10.1016/j.cemconcomp.2010.09.007.
[17] N. U. Kockal et T. Ozturan, « Effects of lightweight fly ash aggregate properties on the behavior of lightweight concretes », *Journal of Hazardous Materials*, vol. 179, n° 1, p. 954-965, juill. 2010, doi: 10.1016/j.jhazmat.2010.03.098.
[18] F. K. Alqahtani, M. I. Khan, G. Ghataora, et S. Dirar, « Production of Recycled Plastic Aggregates and Its Utilization in Concrete », *Journal of Materials in Civil Engineering*, vol. 29, n° 4, p. 04016248, avr. 2017, doi: 10.1061/(ASCE)MT.1943-5533.0001765.
[19] M. Franus, R. Panek, J. Madej, et W. Franus, « The properties of fly ash derived lightweight aggregates obtained using microwave radiation », *Construction and Building Materials*, vol. 227, p. 116677, déc. 2019, doi: 10.1016/j.conbuildmat.2019.116677.
[20] M. Benali, V. Gerbaud, et M. Hemati, « Effect of operating conditions and physico–chemical properties on the wet granulation kinetics in high shear mixer », *Powder Technology*, vol. 190, n° 1, p. 160-169, mars 2009, doi: 10.1016/j.powtec.2008.04.082.
[21] K. P. Hapgood et B. Khanmohammadi, « Granulation of hydrophobic powders », *Powder Technology*, vol. 189, n° 2, p. 253-262, janv. 2009, doi: 10.1016/j.powtec.2008.04.033.
[22] M. Singh, S. Shirazian, V. Ranade, G. M. Walker, et A. Kumar, « Challenges and opportunities in modelling wet granulation in pharmaceutical industry – A critical review », *Powder Technology*, vol. 403, p. 117380, mai 2022, doi: 10.1016/j.powtec.2022.117380.
[23] L. Vandevivere, E. Van Wijmeersch, O. Häusler, T. De Beer, C. Vervaet, et V. Vanhoorne, « The effect of screw configuration and formulation variables on liquid requirements and granule quality in a continuous twin screw wet granulation process », *Journal of Drug Delivery Science and Technology*, vol. 68, p. 103042, févr. 2022, doi: 10.1016/j.jddst.2021.103042.
[24] S. M. Iveson, J. D. Litster, K. Hapgood, et B. J. Ennis, « Nucleation, growth and breakage phenomena in agitated wet granulation processes: a review », *Powder Technology*, vol. 117, n° 1, p. 3-39, juin 2001, doi: 10.1016/S0032-5910(01)00313-8.
[25] V. Chouk, G. Reynolds, M. Hounslow, et A. Salman, « Single drop behaviour in a high shear granulator », *Powder Technology*, vol. 189, n° 2, p. 357-364, janv. 2009, doi: 10.1016/j.powtec.2008.04.019.
[26] P. K. Le, P. Avontuur, M. J. Hounslow, et A. D. Salman, « The kinetics of the granulation process: Right from the early stages », *Powder Technology*, vol. 189, n° 2, p. 149-157, janv. 2009, doi: 10.1016/j.powtec.2008.04.018.

[27] P. B. Pathare, N. Baş, J. J. Fitzpatrick, K. Cronin, et E. P. Byrne, « Effect of high shear granulation process parameters on the production of granola cereal aggregates », *Biosystems Engineering*, vol. 110, n° 4, p. 473-481, déc. 2011, doi: 10.1016/j.biosystemseng.2011.10.004.
[28] P. Pandey, J. Tao, A. Chaudhury, R. Ramachandran, J. Z. Gao, et D. S. Bindra, « A combined experimental and modeling approach to study the effects of high-shear wet granulation process parameters on granule characteristics », *Pharmaceutical Development and Technology*, vol. 18, n° 1, p. 210-224, févr. 2013, doi: 10.3109/10837450.2012.700933.
[29] S. I. F. Badawy, M. M. Menning, M. A. Gorko, et D. L. Gilbert, « Effect of process parameters on compressibility of granulation manufactured in a high-shear mixer », *International Journal of Pharmaceutics*, vol. 198, n° 1, p. 51-61, mars 2000, doi: 10.1016/S0378-5173(99)00445-7.
[30] C. Mangwandi, M. J. Adams, M. J. Hounslow, et A. D. Salman, « Effect of impeller speed on mechanical and dissolution properties of high-shear granules », *Chemical Engineering Journal*, vol. 164, n° 2, p. 305-315, nov. 2010, doi: 10.1016/j.cej.2010.05.039.
[31] M. Bardin, P. C. Knight, et J. P. K. Seville, « On control of particle size distribution in granulation using high-shear mixers », *Powder Technology*, vol. 140, n° 3, p. 169-175, févr. 2004, doi: 10.1016/j.powtec.2004.03.003.
[32] N. Rahmanian, A. Naji, et M. Ghadiri, « Effects of process parameters on granules properties produced in a high shear granulator », *Chemical Engineering Research and Design*, vol. 89, n° 5, p. 512-518, mai 2011, doi: 10.1016/j.cherd.2010.10.021.
[33] M. X. L. Tan et K. P. Hapgood, « Foam granulation: Effects of formulation and process conditions on granule size distributions », *Powder Technology*, vol. 218, p. 149-156, mars 2012, doi: 10.1016/j.powtec.2011.12.006.
[34] P. C. Knight, A. Johansen, H. G. Kristensen, T. Schæfer, et J. P. K. Seville, « An investigation of the effects on agglomeration of changing the speed of a mechanical mixer », *Powder Technology*, vol. 110, n° 3, p. 204-209, juin 2000, doi: 10.1016/S0032-5910(99)00259-4.
[35] J. G. Jang et H. K. Lee, « Microstructural densification and CO2 uptake promoted by the carbonation curing of belite-rich Portland cement », *Cement and Concrete Research*, vol. 82, p. 50-57, avr. 2016, doi: 10.1016/j.cemconres.2016.01.001.
[36] A. el M. Safhi, P. Rivard, A. Yahia, K. Henri Khayat, et N.-E. Abriak, « Durability and transport properties of SCC incorporating dredged sediments », *Construction and Building Materials*, vol. 288, p. 123116, juin 2021, doi: 10.1016/j.conbuildmat.2021.123116.
[37] L. Van Ginneken, V. Dutré, W. Adriansens, et H. Weyten, « Effect of liquid and supercritical carbon dioxide treatments on the leaching performance of a cement-stabilised waste form », *The Journal of Supercritical Fluids*, vol. 30, n° 2, p. 175-188, juill. 2004, doi: 10.1016/j.supflu.2003.07.004.
[38] AFNOR, « EN 13055-1, Lightweight aggregates for concrete, mortar and grou », décembre 2002.
[39] Y. Mamindy-Pajany, C. Hurel, N. Marmier, et M. Roméo, « Arsenic (V) adsorption from aqueous solution onto goethite, hematite, magnetite and zero-valent iron: Effects of pH, concentration and reversibility », *Desalination*, vol. 281, p. 93-99, oct. 2011, doi: 10.1016/j.desal.2011.07.046.
[40] AFNOR, « NF EN ISO 18757, Determination of specific surface area pf ceramic powders by gas adsorption using the BET method », juin 2006.
[41] AFNOR, « NF EN 1097-7 “Tests for mechanical and physical properties for aggresgates” », juin 2008.
[42] AFNOR, « NF ISO 13320-1, Laser diffraction methods », septembre 2000.
[43] AFNOR, « NF EN 933-1 “Test for geometrical properties of aggresgates”. », mai 2012.
[44] AFNOR, « NF EN 933-2 “Test for geometrical properties of aggresgates”. », juin 2020.
[45] AFNOR, « NF EN 12457-2, Leaching-Compliance test for leaching of granular wasre materials ans sludges », décembre 2002.
[46] AFNOR, « ASTM C 618, Standard Specification for Coal Fly Ash and Raw or Calcined Natural Pozzolan for Use in Concrete », décembre 2002.

[47] I.-J. Chiou, K.-S. Wang, C.-H. Chen, et Y.-T. Lin, « Lightweight aggregate made from sewage sludge and incinerated ash », *Waste Management*, vol. 26, n° 12, p. 1453-1461, janv. 2006, doi: 10.1016/j.wasman.2005.11.024.
[48] M. Criado, A. Palomo, et A. Fernández-Jiménez, « Alkali activation of fly ashes. Part 1: Effect of curing conditions on the carbonation of the reaction products », *Fuel*, vol. 84, n° 16, p. 2048-2054, nov. 2005, doi: 10.1016/j.fuel.2005.03.030.
[49] AFNOR, « NF EN 1097-3 “Tests for mechanical and physical properties of aggregates” », août 1998.
[50] AFNOR, « NF P 94-410-3 “Essais pour déterminer les propriétés physiques des roches” », mai 2001.
[51] AFNOR, « EN 1097-6 “Tests for mechanical and physical properties of aggregates” », février 2022.
[52] AFNOR, « NF EN 1744-1+A1 “Tests for chemical properties of aggregates” », février 2014.
[53] Y. Liu, D. Scharf, T. Graule, et F. J. Clemens, « Granulation processing parameters on the mechanical properties of diatomite-based porous granulates », *Powder Technology*, vol. 263, p. 159-167, sept. 2014, doi: 10.1016/j.powtec.2014.04.094.
[54] G. M. Walker, « Chapter 4 Drum Granulation Processes », in *Handbook of Powder Technology*, vol. 11, A. D. Salman, M. J. Hounslow, et J. P. K. Seville, Éd. Elsevier Science B.V., 2007, p. 219-254. doi: 10.1016/S0167-3785(07)80039-X.
[55] J. J. Dijkstra, H. A. van der Sloot, et R. N. J. Comans, « The leaching of major and trace elements from MSWI bottom ash as a function of pH and time », *Applied Geochemistry*, vol. 21, n° 2, p. 335-351, févr. 2006, doi: 10.1016/j.apgeochem.2005.11.003.
[56] A. Bouchikhi, A. el M. Safhi, P. Rivard, R. Snellings, et N.-E. Abriak, « Fluvial Sediments as SCMs: Characterization, Pozzolanic Performance, and Optimization of Equivalent Binder », *Journal of Materials in Civil Engineering*, vol. 34, n° 2, p. 04021430, 2022.
[57] F. Casini, G. M. B. Viggiani, et S. M. Springman, « Breakage of an artificial crushable material under loading », *Granular Matter*, vol. 15, n° 5, p. 661-673, oct. 2013, doi: 10.1007/s10035-013-0432-x.
[58] R. F. Rodrigues, S. R. Leite, D. A. Santos, et M. A. S. Barrozo, « Drum granulation of single super phosphate fertilizer: Effect of process variables and optimization », *Powder Technology*, vol. 321, p. 251-258, nov. 2017, doi: 10.1016/j.powtec.2017.08.036.
[59] H. A. van der Sloot, R. N. J. Comans, et O. Hjelmar, « Similarities in the leaching behaviour of trace contaminants from waste, stabilized waste, construction materials and soils », *Science of The Total Environment*, vol. 178, n° 1, p. 111-126, janv. 1996, doi: 10.1016/0048-9697(95)04803-0.
[60] S.-Y. Pan, E. E. Chang, et P.-C. Chiang, « CO2 Capture by Accelerated Carbonation of Alkaline Wastes: A Review on Its Principles and Applications », *Aerosol Air Qual. Res.*, vol. 12, n° 5, p. 770-791, 2012, doi: 10.4209/aaqr.2012.06.0149.
[61] E. Rendek, G. Ducom, et P. Germain, « Carbon dioxide sequestration in municipal solid waste incinerator (MSWI) bottom ash », *Journal of Hazardous Materials*, vol. 128, n° 1, p. 73-79, janv. 2006, doi: 10.1016/j.jhazmat.2005.07.033.
[62] P. J. Gunning, C. D. Hills, et P. J. Carey, « Accelerated carbonation treatment of industrial wastes », *Waste management*, vol. 30, n° 6, p. 1081-1090, 2010.
[63] H. Ecke, N. Menad, et A. Lagerkvist, « Carbonation of Municipal Solid Waste Incineration Fly Ash and the Impact on Metal Mobility », *Journal of Environmental Engineering*, vol. 129, n° 5, p. 435-440, mai 2003, doi: 10.1061/(ASCE)0733-9372(2003)129:5(435).
[64] V. Ducman, A. Mladenovič, et J. S. Šuput, « Lightweight aggregate based on waste glass and its alkali–silica reactivity », *Cement and Concrete Research*, vol. 32, n° 2, p. 223-226, févr. 2002, doi: 10.1016/S0008-8846(01)00663-9.
[65] B. González-Corrochano, J. Alonso-Azcárate, M. Rodas, F. J. Luque, et J. F. Barrenechea, « Microstructure and mineralogy of lightweight aggregates produced from washing aggregate

sludge, fly ash and used motor oil », *Cement and Concrete Composites*, vol. 32, nº 9, p. 694-707, oct. 2010, doi: 10.1016/j.cemconcomp.2010.07.014.
[66] B. González-Corrochano, J. Alonso-Azcárate, M. Rodas, J. F. Barrenechea, et F. J. Luque, « Microstructure and mineralogy of lightweight aggregates manufactured from mining and industrial wastes », *Construction and Building Materials*, vol. 25, nº 8, p. 3591-3602, août 2011, doi: 10.1016/j.conbuildmat.2011.03.053.
[67] P. Monteiro, *Concrete: microstructure, properties, and materials*. McGraw-Hill Publishing, 2006.
[68] L. A. Bui, C. Hwang, C. Chen, K. Lin, et M. Hsieh, « Manufacture and performance of cold bonded lightweight aggregate using alkaline activators for high performance concrete », *Construction and Building Materials*, vol. 35, p. 1056-1062, oct. 2012, doi: 10.1016/j.conbuildmat.2012.04.032.
[69] B. González-Corrochano, J. Alonso-Azcárate, et M. Rodas, « Characterization of lightweight aggregates manufactured from washing aggregate sludge and fly ash », *Resources, Conservation and Recycling*, vol. 53, nº 10, p. 571-581, août 2009, doi: 10.1016/j.resconrec.2009.04.008.
[70] B. González-Corrochano, J. Alonso-Azcárate, et M. Rodas, « Production of lightweight aggregates from mining and industrial wastes », *Journal of Environmental Management*, vol. 90, nº 8, p. 2801-2812, juin 2009, doi: 10.1016/j.jenvman.2009.03.009.
[71] C. Ferone, F. Colangelo, F. Messina, F. Iucolano, B. Liguori, et R. Cioffi, « Coal Combustion Wastes Reuse in Low Energy Artificial Aggregates Manufacturing », *Materials*, vol. 6, nº 11, Art. nº 11, nov. 2013, doi: 10.3390/ma6115000.
[72] L. H. Nguyen, A.-L. Beaucour, S. Ortola, et A. Noumowé, « Influence of the volume fraction and the nature of fine lightweight aggregates on the thermal and mechanical properties of structural concrete », *Construction and Building Materials*, vol. 51, p. 121-132, janv. 2014, doi: 10.1016/j.conbuildmat.2013.11.019.
[73] R. C. Valore, « Calculations of U-Values of Hollow Concrete Masonry », *Concrete International*, vol. 2, nº 2, p. 40-63, févr. 1980.
[74] T. Van Gerven, J. Moors, V. Dutré, et C. Vandecasteele, « Effect of CO2 on leaching from a cement-stabilized MSWI fly ash », *Cement and Concrete Research*, vol. 34, nº 7, p. 1103-1109, juill. 2004, doi: 10.1016/j.cemconres.2003.11.022.
[75] M. S. Abrams et A. H. Gustaferro, « FIRE ENDURANCE OF CONCRETE SLABS AS INFLUENCED BY THICKNESS, AGGREGATE TYPE, AND MOISTURE », *Portland Cement Assoc R & D Lab Bull*, nº 0, Art. nº No 223, 2021.

Declaration of Competing Interest

The authors declare that they have no known competing financial interests or personal relationships that could have appeared to influence the work reported in this paper. The manuscript has not been submitted to a preprint server prior to submission on Powder Technology.

The authors declare that no funds, grants, or other support were received during the preparation of this manuscript

The authors have no relevant financial or non-financial interests to disclose

All authors contributed to the study conception and design. Material preparation, data collection and analysis were performed by Bader Bouzar and Yannick Mamindy-Pajany.

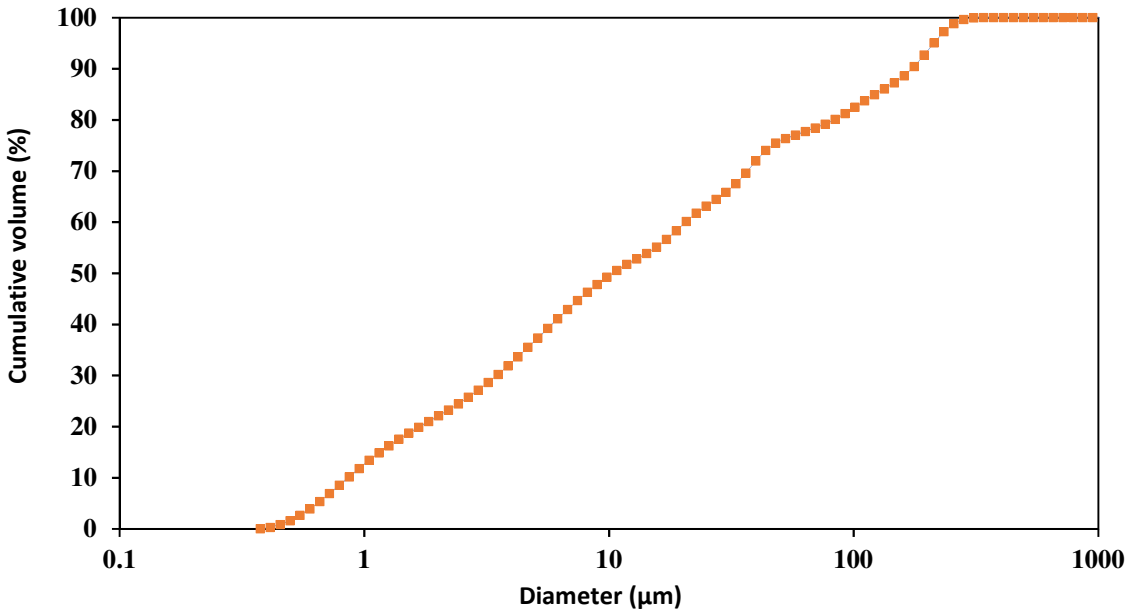

Fig. 1. Granular distributions of WPFA.

Fig.2. Eirich high-intensity granulator

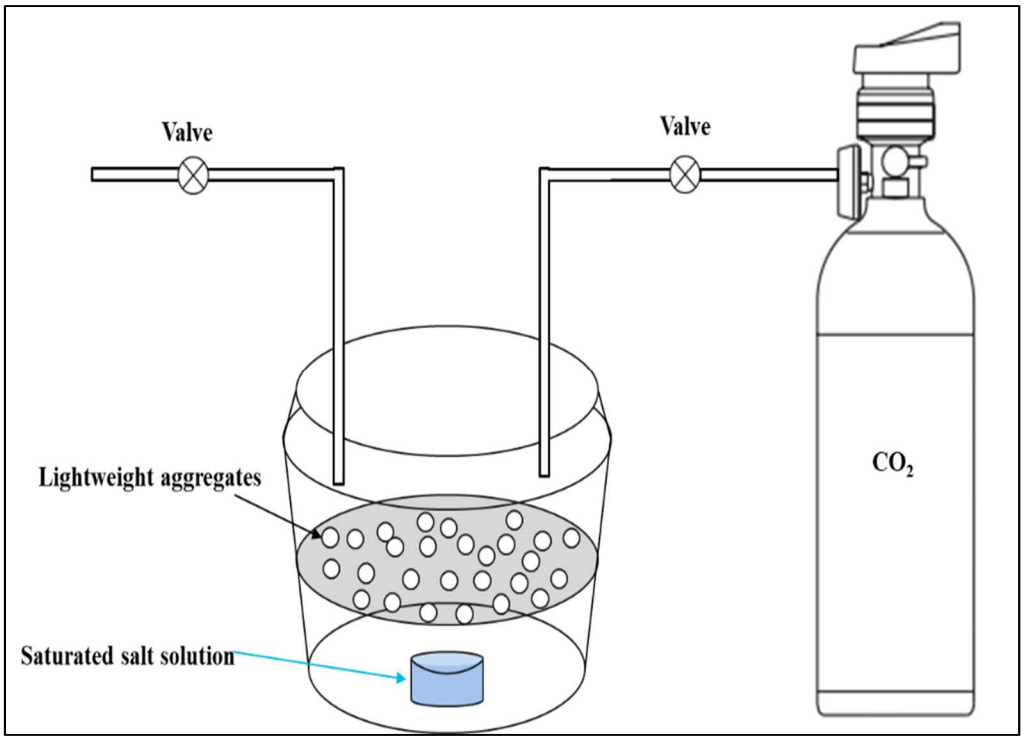

Fig.3 LWA carbonation apparatus

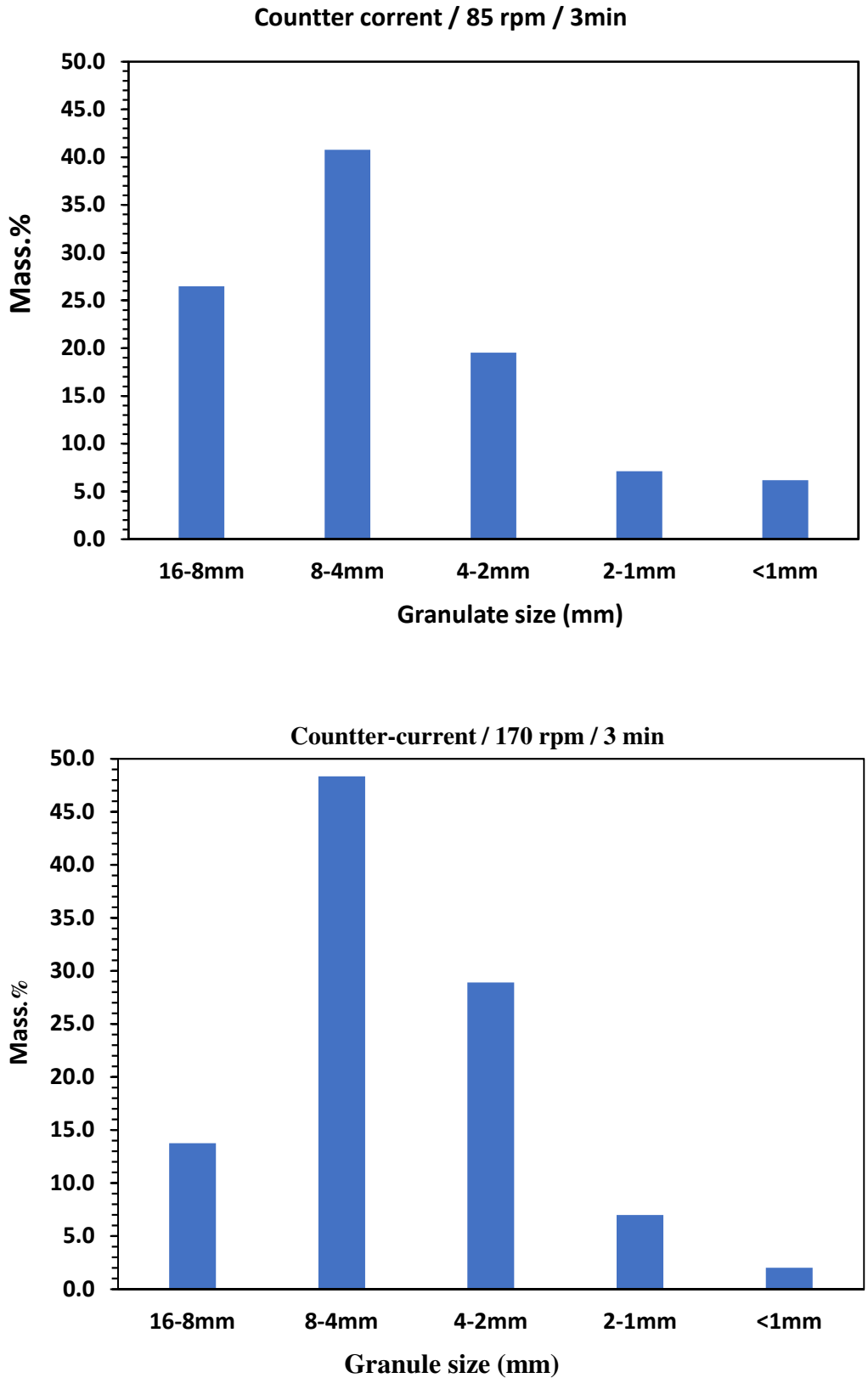

Fig.4 Size distribution for LWA fabricated under counter current rotation mode

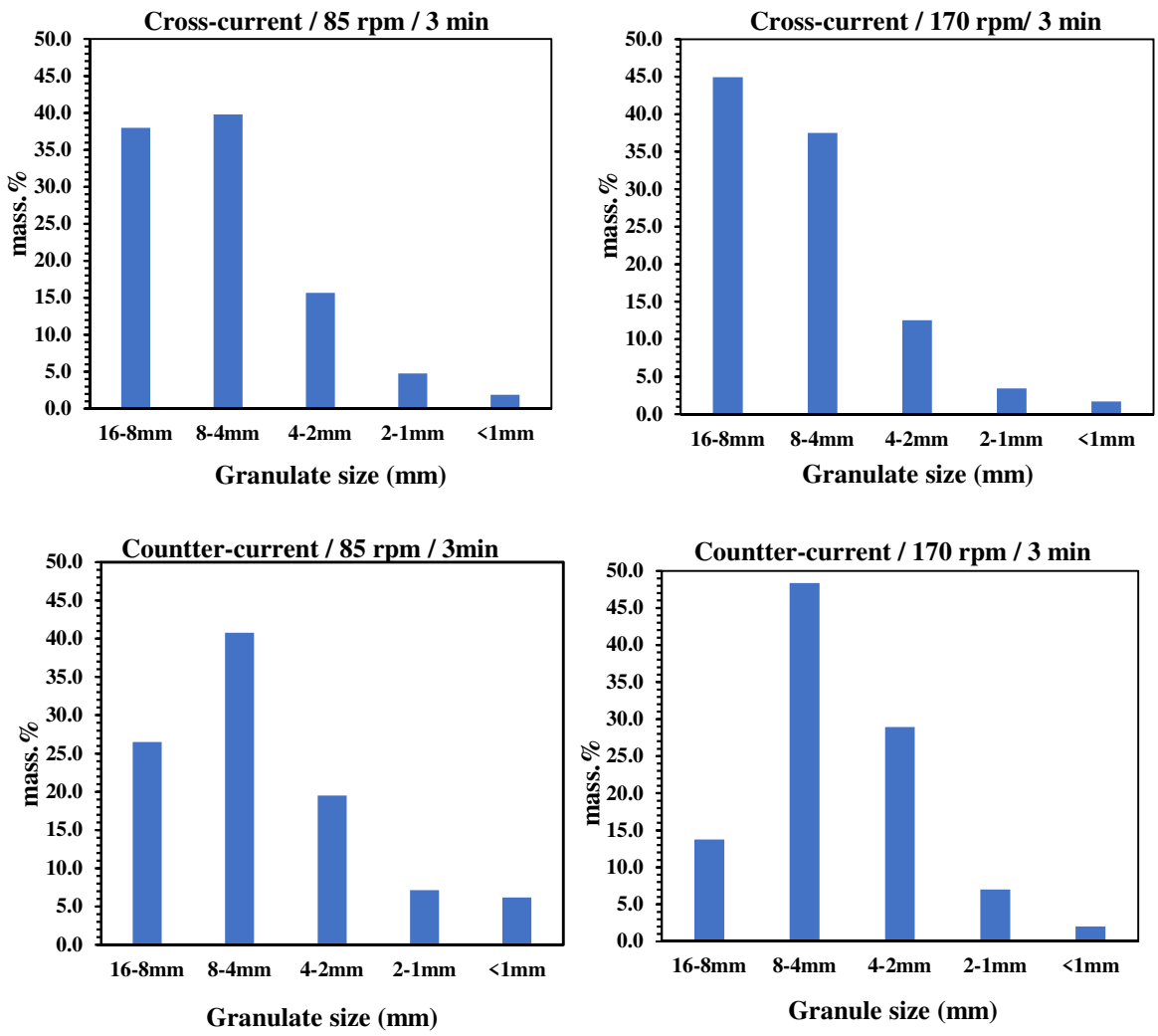

Fig.5 Size distribution of LWA fabricated under different rotation modes

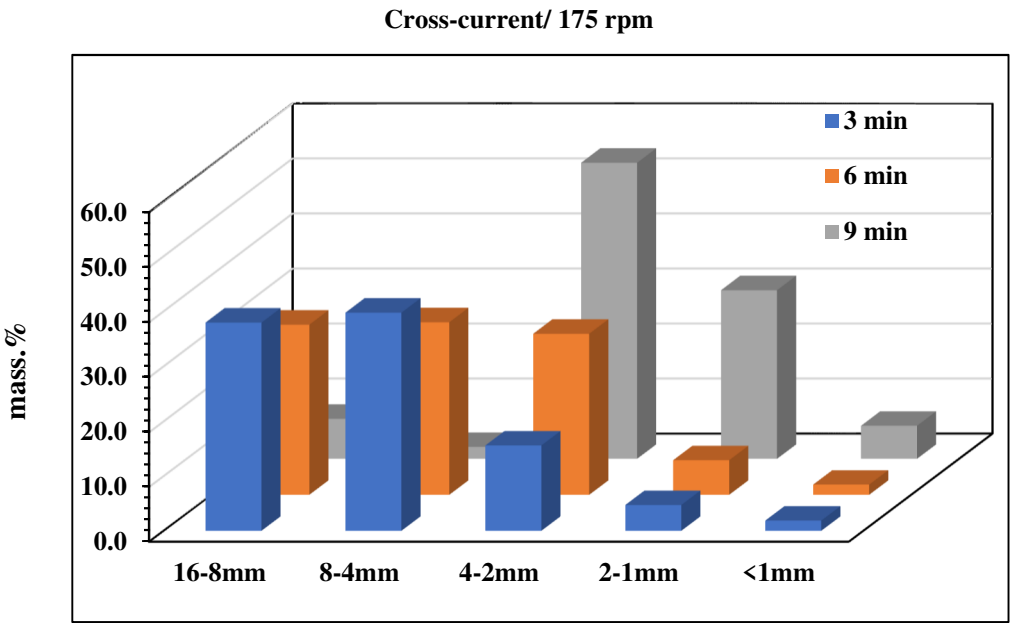

Fig. 6. Effect of the granulation time on the size distribution of LWA produced.

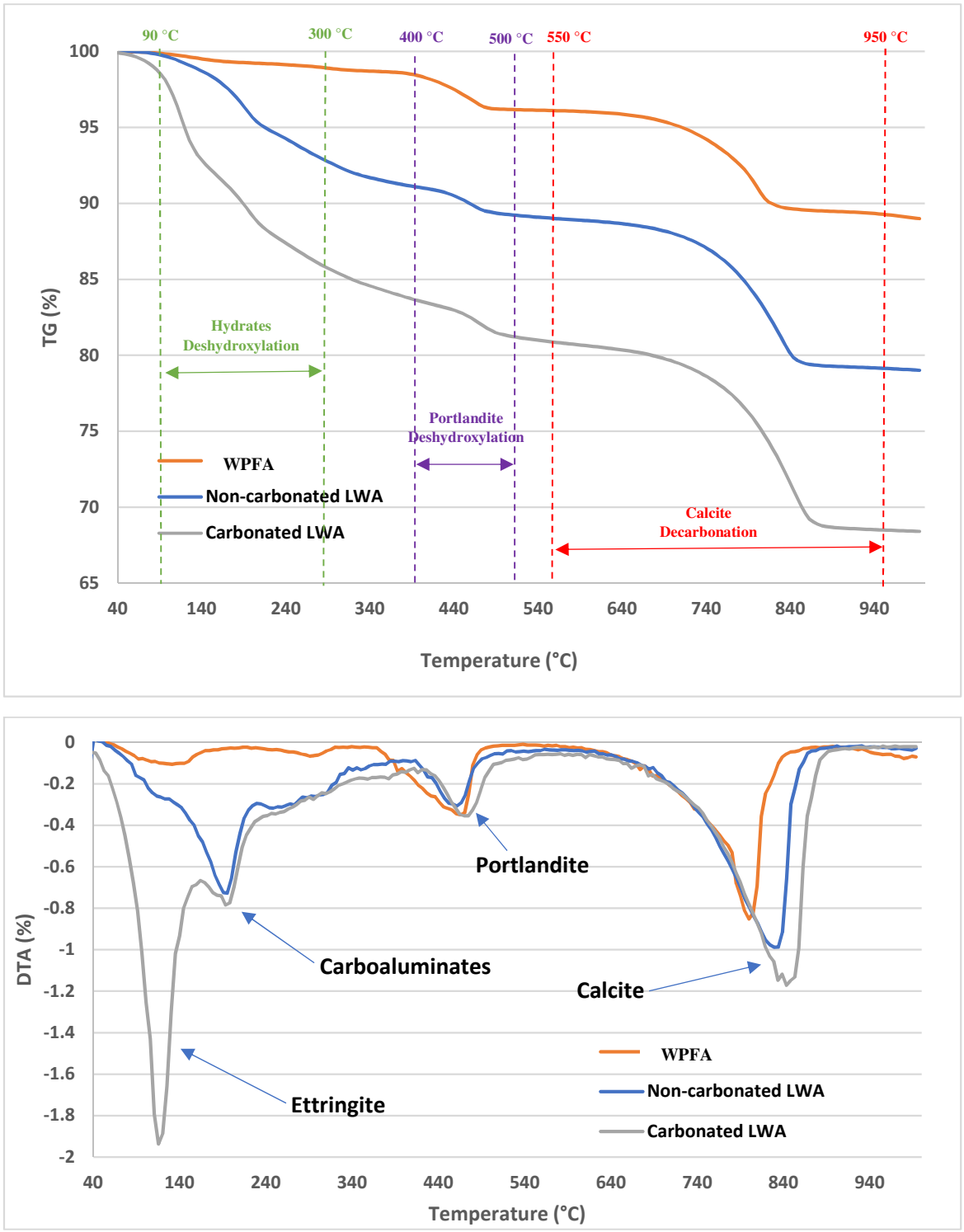

Fig 7. The thermal characteristics of the WPFA and LWA before and after carbonation

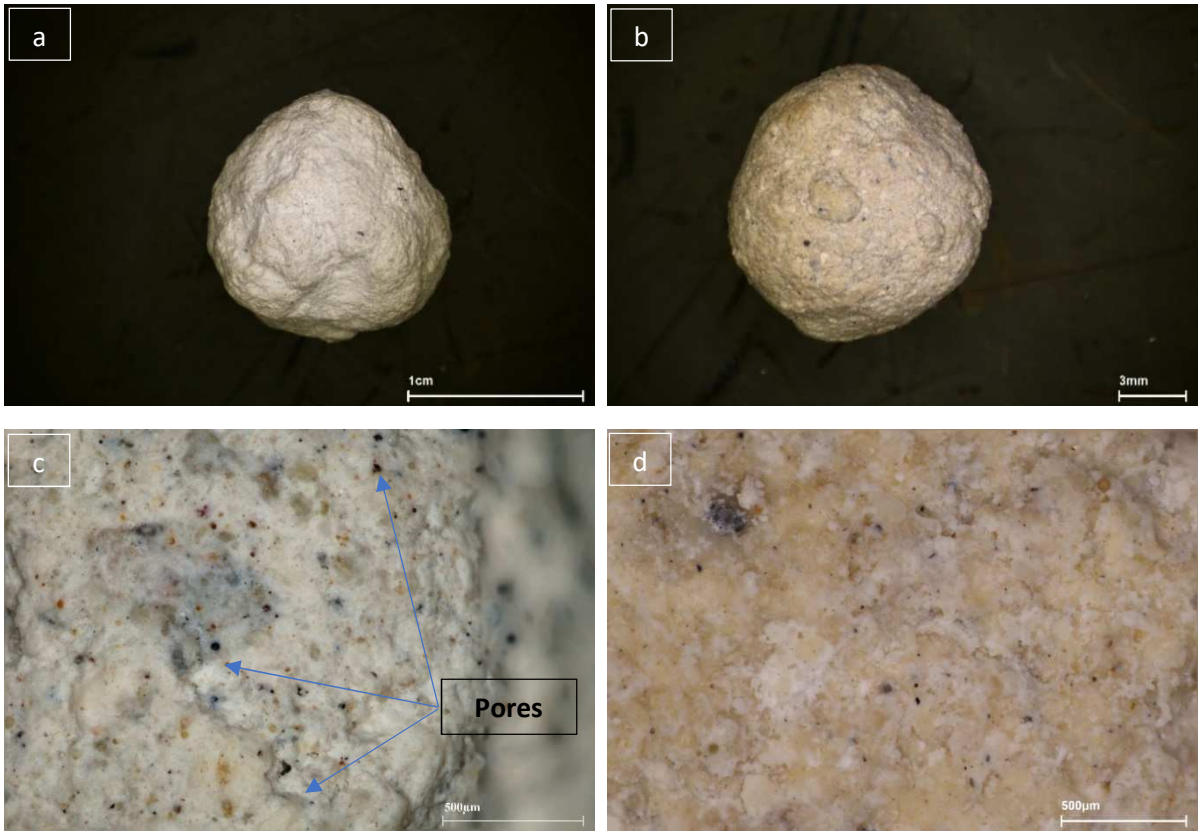

Fig.8. Optical images of the LWA made by from WPFA before **(a,c)** and after **(b,d)** carbonation (Zeiss digital microscope)

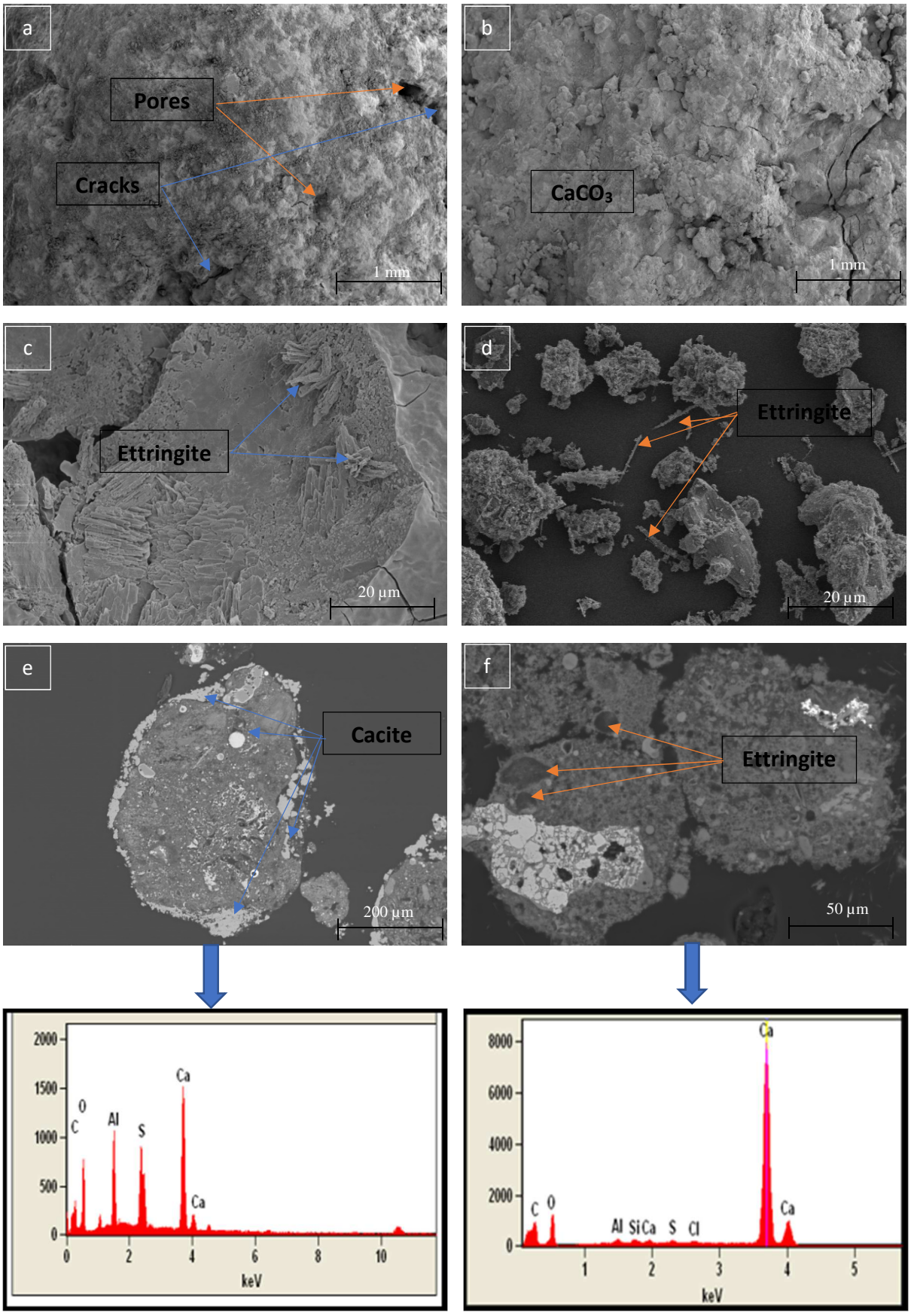

Fig.9. SEM-EDS picture of the LWA before **(a)** and after **(b)**, **(c)**, **(d), (e), (f)** carbonation

Chemical composition by XRF	wt.%	Metallic and metalloids trace elements (MMTE)	Concentration ($mg.kg^{-1}$)
SiO_2	14.59	As	<0.11
Al_2O_3	8.4	Ba	178±6
MgO	1.74	Cd	<0.009
Fe_2O_3	0.8	Co	<0.009
CaO	64.02	Cr	<0.011
Na_2O	0.45	Cu	0.09±0.02
SO_3	1.57	Mo	0.08±0.02
TiO_2	0.7	Ni	<0.047
ZnO	0.22	Pb	7.35±0.6
Cl	0.8	Sb	<0.057
BaO	0.11	Se	<0.08
P_2O_5	0.35	Zn	1.1±0.2
K_2O	0.7	Cl	1422±72

Table 1. Chemical composition in major and MMTE of the WPFA.

Physical parameters	Standard	WPFA
Specific density (kg/m^3)	NF EN 1097-7	2980
Median diameter d_{50} (µm)	NF ISO 13320-1	10
Specific surface BET (m^2/kg)	NF EN ISO-18757	2261
pH	NF EN 14429	13.5
Conductivity (mS/cm)	EN 12457-2	11.3
Loss On Ignition (LOI) (%)	EN 12457-2	5.7

Table 2. Physical and chemical characterizations of WPFA

Properties %	ASTM C 618 (Class-C) %	WPFA used
$SiO_2 + Al_2O_3 + Fe_2O_3$	> 50	87.01
SO_3	< 5	1.57
$Na_2O + 0.658K_2O$	< 1.5	0.91
Moisture content	< 3	0
Loss on ignition	< 6	5.7

Table 3. Chemical properties of WPFA and specification requirements.

Experimental	Rotation modes	Time (min)	Steel pan rotation speeds (rpm)
1	Cross current rotation	3	85
2	Cross current rotation	3	170
3	Counter current rotation	3	85
4	Counter current rotation	3	170
5	Cross current rotation	6	170
6	Cross current rotation	9	170

Table 4. The different granulation parameters of the WPFA.

Concentration (mg/kg)	IWSI	WPFA	Carbonated LWA
As	0.5	<0.11	<0.11
Ba	20	178±6	0.3±0.05
Cd	0.04	<0.009	<0.009
Cr	0.5	<0.011	<0.011
Cu	2	0.09±0.02	0.09±0.02
Mo	0.5	0.08±0.02	0.09±0.03
Ni	0.4	<0.047	<0.047
Pb	0.5	7.35±0.6	<0.03
Sb	0.06	<0.057	<0.057
Se	0.1	<0.08	<0.08
Zn	4	1.1±0.2	<0.01
Chlorides	800	1422±72	1328±48
Fluorides	10	1.1±0.5	-
Sulfates	1000	208±25	206±27
Soluble fraction	4000	3920±121	3980±130
Conductivity ($mS.cm^{-1}$)	***	11.3±0.2	11.8±0.2
pH	***	13.5±0.3	10.4±0.3

Table 5. Concentration (mg/kg) of MMTE in WPFA and Carbonated LWA

Technical specifications	Units	Standard	Non-carbonated LWA	Carbonated LWA	LWA(Argex)
Aggregate form	-	-	Round	Round	Round
Granular class	mm	EN 933-1	2-16	2-16	2-16
Absolute density	(kg/m^3) (±15%)		2105	2370	---
Bulk density	(kg/m^3) (±15%)	EN 1097-3	897	902	550
Apparent density	(kg/m^3) (±15%)	EN 1097-3	1024	1039	---
Compressive strength	MPa (±10%)	EN 13055-1	3.15	7.6	4.7
Crushed particles	% Weight (±15%)	EN 933-5	16.9	14.4	7
Chlorides	% Cl^-	EN 1744-1	0.52	0.49	<0.004
Sulfates soluble in acid	% SO_3	EN 1744-1	0.41	0.38	<0.05
Total Sulfur	%S	EN 1744-1	0.58	0.54	<0.04
Porosity	%	NF P94-410-3	29	21	---
Water absorption (24h)	% (±10%)	EN 1097-6	27.9	19.8	27.3
Thermal conductivity	(W/m°C)	EN 12667	0.19	0.32	0.14
Loss On Ignition (LOI) (900°C)	%	EN 1744-1	27.2	31.3	---

Table 6. Characterization of LWA according to the standard (NF EN 13055-1)

Graphical abstract